FULL LENGTH ARTICLE

Behavior of corroded bonded fully prestressed and conventional concrete beams

Mohamed Moawad [a,*], Hossam El-Karmoty [b,1], Ashraf El Zanaty [c,2]

[a] Cairo University, Faculty of Engineering, Structural Department, 6 El-Ashmawy, El-Mostashfa Street, El Haram, Giza, Egypt
[b] Housing and Building National Research Center, Dokki, Giza, Egypt
[c] Cairo University, Giza, Cairo, Egypt

Abstract   Prestressed concrete is widely used in the construction buildings. And corrosion of steel is one of the most important and prevalent mechanisms of deterioration for concrete structures. Consequently the capacity of post-tension elements decreased after exposure to corrosion. This study presents results of the experimental investigation of the performance/behavior of bonded fully prestressed and conventional concrete beams, with 40 MPa compressive strength exposed to corrosion. The experimental program of this study consisted of three fully prestressed and two conventional concrete beams with overall dimensions equal to $150 \times 400 \times 4500$ mm. The variables were considered in terms of corrosion exposure effect, prestressed level, and corrosion location effect for fully prestressed beams. Mode of failure, cracking width/distribution, ultimate load and the corresponding deflection of each beam were recorded. The results showed that the fully prestressed beam in comparison with conventional beam was considered to be even more resistance to corrosion because it was perceived to be crack-free as a result of prestressing. Also the mention deterioration incident in fully prestressed beams fully corrosion exposure level unnoticed that deterioration incident in partially corrosion exposure level. The most of deterioration incident in fully prestressed beam acts on compression of non-prestressed steel reinforcement. Because the bonded tendons are less likely to corrode. Cement grout/duct is a barrier to moisture and chloride penetration,

* Corresponding author. Tel.: +20 (974)50130851.
E-mail addresses: msmmah83@yahoo.com (M. Moawad), hoskarmoty@yahoo.com (H. El-Karmoty), drashrafzanaty@yahoo.com (A. El Zanaty).
[1] Tel.: +20 1004402981.
[2] Tel.: +20 1223158005.

Production and hosting by Elsevier

Introduction

Many concrete structures suffer from reinforcing steel corrosion especially in marine environments. The concrete structures experience unacceptable loss in load carrying capacity, stiffness and ductility. Many researchers have attempted to characterize the behavior of prestressed concrete beams and corrosion damaged R.C elements.

Omnia [1], studied the behavior of fully and partially prestressed concrete beams and concluded that the presence of the prestressing force delays the concrete cracking and increases the initial stiffness. Ismail [2], studied the behavior of statically determinate prestressed concrete beams subject to fire and concluded that the partially prestressed concrete beams with concrete cover equal to 25 mm have higher resistance to fire exposure than that of fully prestressed concrete beam in terms of ultimate capacity and ductility. Also the high strength of partially and fully prestressed concrete beams had lower fire resistance than normal strength beams.

El-Hefnawy [3], conducted another experimental study on carbonation depth. He measured the carbonation depth for concrete of 18 months age for specimens with/without silica fume by treating a freshly broken concrete surface by phenolphthalein. He found that the addition of silica fume as a partial replacement of cement increases its tendency to react with carbon dioxide in the atmosphere. El-Hefnawy [4], conducted experimental and theoretical study to estimate the residual ultimate capacity of reinforced concrete beams exposed to different degrees of corrosion. EL-hefnawy found that corrosion-induced cracks were unrelated to the degree of rebar corrosion. In addition, he noticed also that none of the tested beams, even severally corroded beams, suffered from spalling of concrete cover. In the theoretical study and because of the irregular shape of the corroded rebar, a statistical approach based on ISO-12491-1997 [5] was carried out to estimate the probable minimum area of the corroded rebar (AF) using four diameters measured at four different random locations along corroded rebar length. Gestsdottir and Gudmundsson [6], investigated bond behavior of naturally corroded reinforcement in concrete structures. The experiments showed that higher degree of corrosion leads to decrease in ultimate load and longer available anchorage length leads to increase in ultimate load. Furthermore the ultimate load is not connected at what load shear or flexural crack forms, and the free end slip of the main bars starts at a load of 90–97% of the maximum load. AL-Attar and Abdul-kareem [7], investigated the influence of chloride ions source on corrosion of steel embedded introduction in different exposures to the external chloride increase in both total and free chloride inside the concrete specimens; the results indicate that the ratio between (CL_{free}/CL_{total}) for high performance concrete mixes is always less by about 76–82% than that of normal concrete mixes and this could be caused by using high cement content and meta-

kaolin. Khafaga and Bahaa [8], investigated the structural behavior of reinforced concrete beams initially deteriorated by corrosion of web reinforcement through an experimental program that comprised tests of eight large-scale beams. The results indicated that corrosion of web reinforcement adversely affected the structural performance of the reinforced concrete beams in terms of strength, stiffness, and ductility. Deterioration of the concrete cover was observed and was more severe for beams reinforced with closely spaced stirrups. Losses in the yield and ultimate capacities up to 36% were recorded. Elgabry et al. [9] investigated the behavior of reinforced concrete frames exposed to corrosion of steel bars and repaired using CFRP. Corrosion of reinforcement steel leads to reduction in ultimate load capacity, stiffness and ductility of the corroded R.C frames. Rehabilitation using CFRP resulted in enhancement in ultimate load carrying capacity up to 44.7%. Using CFRP in rehabilitation of corroded frames limited the propagation of the cracks and increased the cracking load significantly.

Research program

Experimental program

The experimental program consists of testing five beams with overall width, depth and length of 150 mm, 400 mm and 4500 mm respectively, and the beams were simply supported with a clear span of 4200 mm, as shown in Fig. 1. The top longitudinal reinforcement of all specimens was two 10 mm diameter bars. The stirrups were 10 mm diameter bars every 200 mm at middle part of the beams and every 100 mm at edges for a distance 1400 mm from support to middle span of beam, as shown in Fig. 2. Fig. 3 shows the prestressing strand had a draped profile similar to the shape of the bending moment produced by acting loads. The main reinforcement of the specimens changed according to the prestressing index. One strand with diameter 15.24 mm was used to reinforce the fully prestressed beams and seven 10 mm diameter bars were used to reinforce the non-prestressed beams. Additional horizontal stirrups were added at anchor zone to resist the splitting force, which is produced at the anchor zone; these stirrups were calculated according to recommendation of the Egyptian code [10]. The variables considered in this study are corrosion exposure effect, prestressed level, and corrosion location effect as given in Table 1.

The prestressing strand was placed inside polyethylene duct and fixed with the beam stirrups using horizontal steel chairs. The grouting fitting was placed at distance of 300 mm from each side of beam. The strands were stressed after the concrete had reached an age of 28 days, and then grouted with cementations grout according to specification instructions.

During prestressing, the strand elongation was measured and the prestressing force was recorded. Table 2 shows the
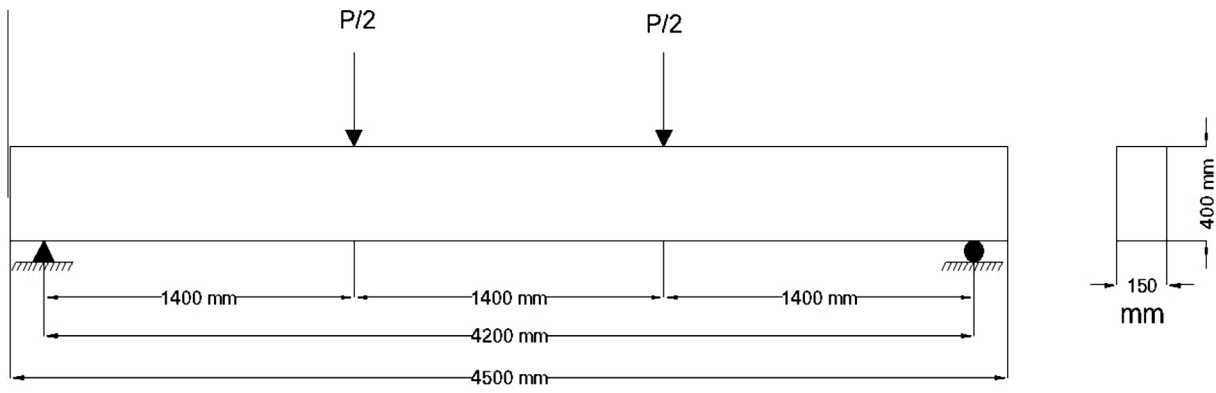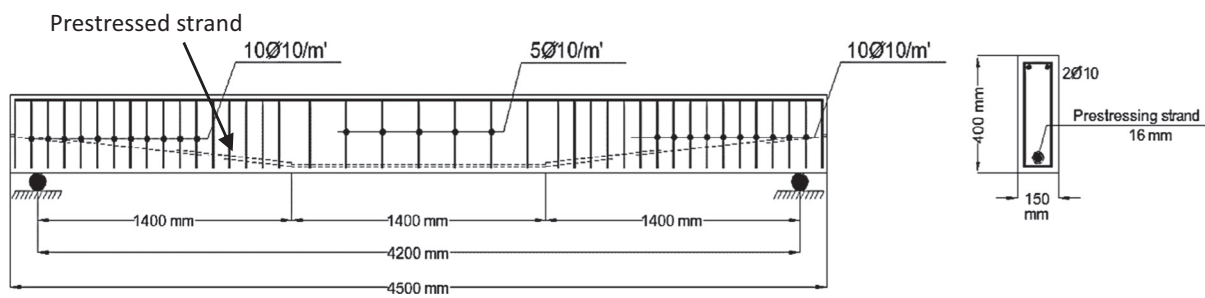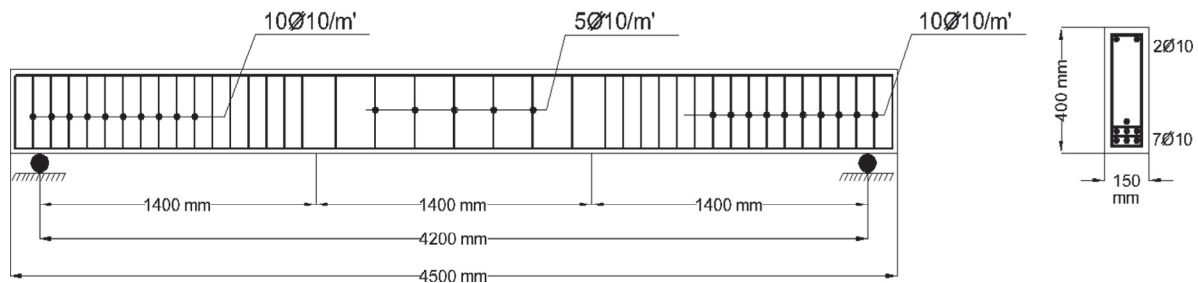
Fig. 1 Concrete dimensions of tested beam.

(a) Reinforcement detail of bonded fully prestressed concrete beams

(b) Reinforcement detail of conventional concrete beams.

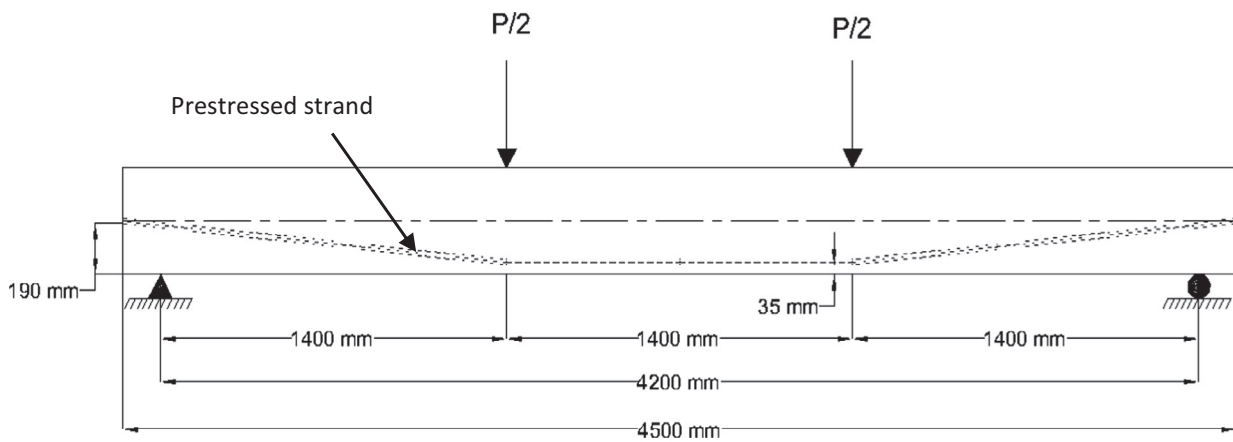Fig. 2 Reinforcement details with stirrup distribution along beam length.

Fig. 3 Prestressed duct profile for 25 mm concrete cover.

Table 1 Experimental program.

SP.	Sample no.	fcu[a] (MPa)	Prestressing index (ip)[b]	Strand diameter (mm)	As	As'	Corrosion cond.	Corrosion location[c]
1	*B1*	42	0.00	–	7T10	2T10	Not exposed	–
2	*B2*	45	0.00	–	7T10	2T10	Exposed	*TE*
3	*B3*	50	1.00	15.24	–	2T10	Not exposed	–
4	*B4*	45	1.00	15.24	–	2T10	Exposed	*FE*
5	*B5*	48	1.00	15.24	–	2T10	Exposed	*PE*

[a] f_{cu} refers to the concrete compressive strength.

[b] ip refer to (Prestressing index) is the ratio of the yield force of the prestressing reinforcement to the sum of the yield force of the prestressing and non-prestressing reinforcement.

[c] (TE, FE and PE) refers to full or partial exposure (tension of non-prestressed steel, compression of non-prestressed and prestressed steel exposed, and prestressed tendon exposed) to corrosion respectively.

Table 2 Jacking force, initial prestressed force and extension value for theoretical and experimental results.

SP.	Specimen	Jacking load (kN)	Theoretical initial load (kN)	Theoretical extension (mm)	Experimental initial load (kN)	Experimental extension (mm)
3–5	Fully prestressed beams	195.3	144.11	23.16	136.89	22

experimentally measured and theoretically calculated force and elongation for bonded fully prestressed beams.

Materials properties

Natural siliceous sand and crushed stone had a nominal maximum size of 10 mm. Ordinary Portland Cement (OPC) and tap drinking water were used in this work. Also super plasticizer admixture Sikament-163 M was used. The admixture complies with the ASTM C 494 type A. Testing of these materials was carried out according to Egyptian Standard Specifications and the ASTM Standards.

Deformed high grade steel bars of 10 mm diameter with yield strength of 470 N/mm^2 and ultimate strength of 610 N/mm^2 were used as stirrups and longitudinal tension and compression reinforcement. Steel bars were tested and comply with Egyptian Standard Specifications.

Fabrication of tested beams

The specimens were fabricated at two stages. The first stage was the casting of three bonded fully prestressed concrete beams and two conventional concrete beams, and then the second stage was the corrosion technic of three beams.

Concrete mix was produced with target compressive strength of 40 MPa after 28 days. The concrete mix proportions are illustrated in Table 3.

Concrete was cast in the material laboratory of Housing and Building National Research Center at 25 °C temperature. Concrete was compacted after casting using an electrical vibrator for two minutes. The sides of the form were removed after 48 h. Curing of specimens started immediately after casting for 7 days.

Accelerated corrosion technique

The first phase of the tests was speeding up the rate of corrosion of the steel reinforcement in order to induce deterioration of the bonded fully prestressed concrete beams and conventional concrete beam. Therefore, two bonded fully prestressed concrete beams and one conventional concrete beam were subjected to the electrochemical accelerated corrosion technique. The corrosion setup consisted of the test specimen, stainless steel plates (acting as an artificial cathode), and a wet medium between the stainless steel plate and the beams, and a D.C. power supply. The wet medium was burlap wetted by 3% NaCl solution. It should be noted that the cathode stainless steel plate was mounted along regular cross-sectional beam as shown in Fig. 4. The value of the applied current intensity was about 10 μA/mm^2 for all of the corroded specimens. This value is considered appropriate for accelerated corrosion tests and has been successfully used by several researchers [3,4,7–9]. The applied current was maintained constant for all specimens by using a variable resistance and was monitored by means of an ammeter.

The corrosion level degree was changed from rough to smooth surface in this research, and it was used the mild degree of corrosion. To achieve this degree of corrosion, the specimens were subjected to the corrosion setup for 120 days.

Test setup

The beams were subjected to two concentrated loads at 700 mm from mid span using two hydraulic jacks of 800 kN capacity. The loads were measured using a load cell of 800 kN capacity, as shown in Fig. 5. The beams were tested

Table 3 Mix design proportions.

Mix	f_{cu} (Mpa)	Cement (kg)	Sand (kg)	Dolomite (kg)	Water (kg)	Silica fume (kg)	Admixture type	Admixture (% of cement weight)
1	40	450	715	1070	200	–	Sikament-163 M	0.9

(a) drainage system for Conventionally concrete beam.

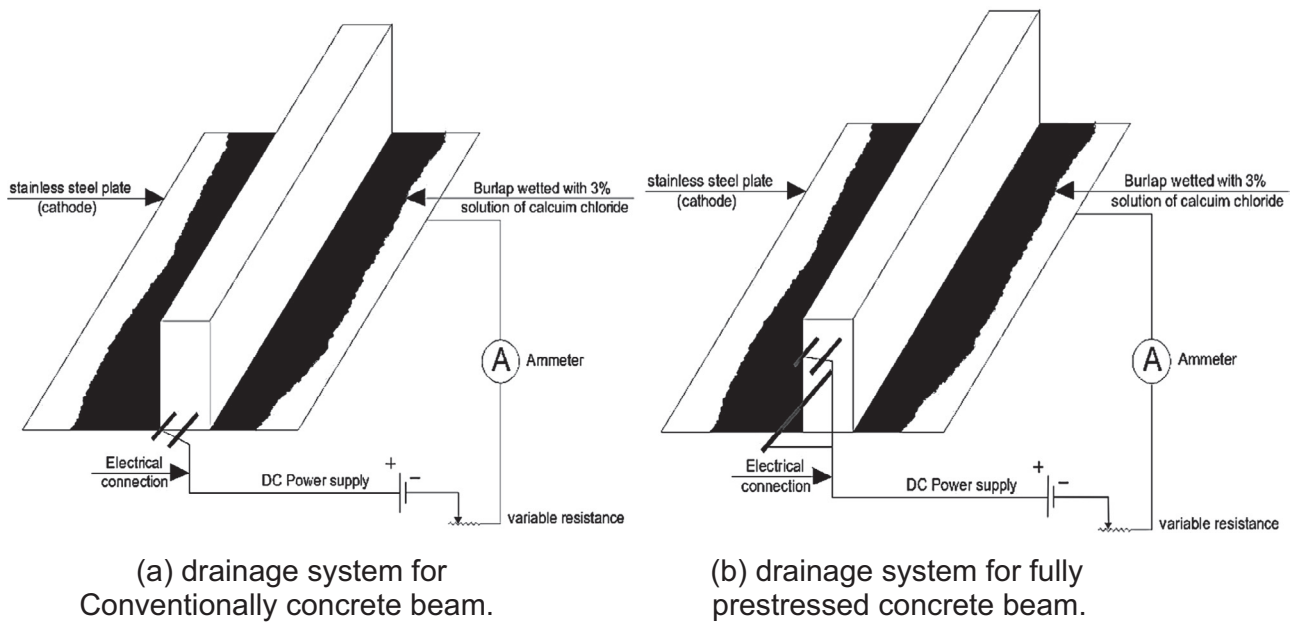(b) drainage system for fully prestressed concrete beam.

Fig. 4   Shows that the drainage system that keeps the media wet for transporting the electrical field in the samples.
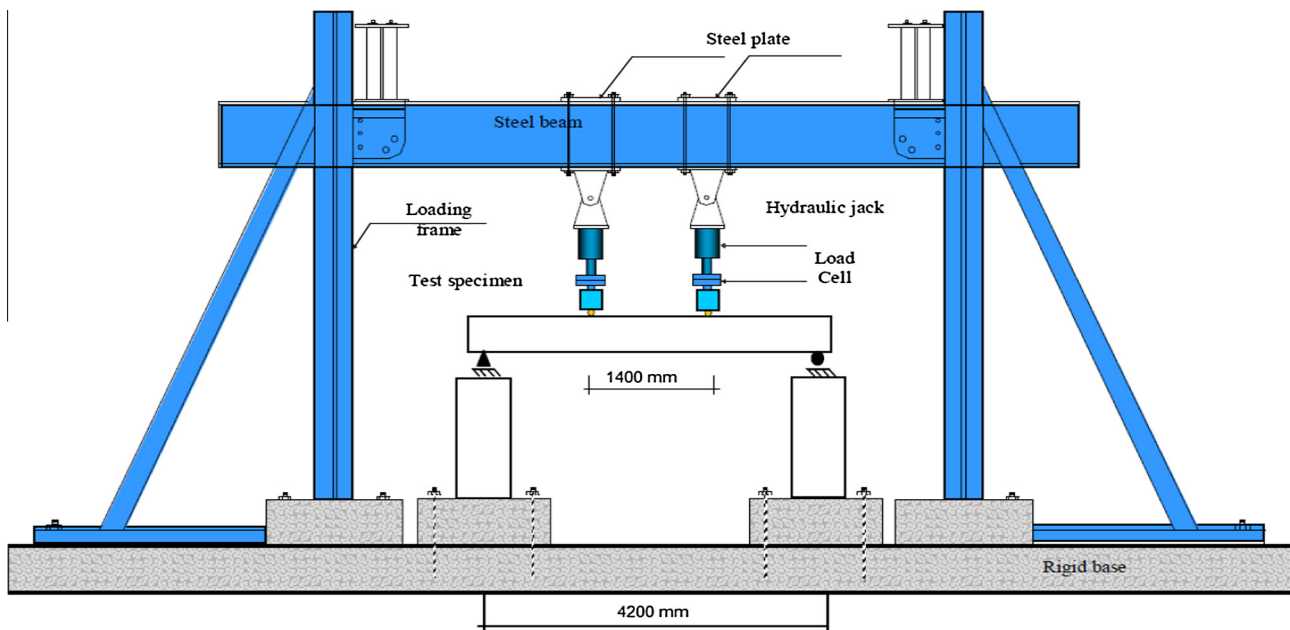

Fig. 5   Test setup for tested beams.

up to failure using a stroke control system. The data were collected using a data acquisition system and "a LabVIEW" software at a rate of 1 record per second. The specimen was supported over two concrete blocks of 1400 mm height using one free rod to simulate a roller support and restrained rod to simulate a hinged support.

Instrumentation

The longitudinal strains of specimens were measured by two different methods: linear variable differential transducers, (LVDT), and electric strain gauges. The strains of concrete

and non-prestressed steel reinforcement were measured in the longitudinal direction. Deflection was measured at mid-span and under the concentrated loads. Fig. 6 shows location of different instrumentations.

Experimental results and analysis

The measured cracking, yielding, ultimate load capacities and the corresponding deflections of each beam are presented in Table 4. Ductility, initial stiffness and post-cracking stiffness of each beam are presented in Table 5.
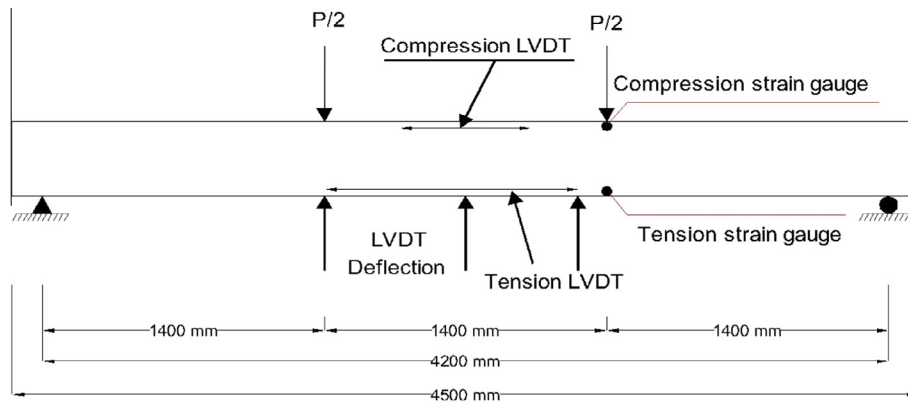
Fig. 6   Location of different instrumentations for tested beams.

Table 4   Results of cracking, yielding, ultimate load capacities and the corresponding deflections of tested specimens.

SP.	Sample name	P_{cr} (kN)	Δ_{cr} (mm)	P_y (kN)	Δ_Y (mm)	P_u (kN)	Δ_U (mm)
1	B1	18	1.8	127	24.5	130	44
2	B2	8	1.85	98	35	106.32	67.8
3	B3	35	2.5	90	51.8	123.8	101
4	B4	25	2.4	78	25	111.36	48
5	B5	45	3.07	112	52	117.27	95

Table 5   Results of ductility, initial stiffness and post-cracking stiffness of tested specimens.

SP.	Sample name	Ductility[a] AU/AY	ki[b]	Ku[c]
1	B1	4.68	10	3.4
2	B2	3.2	4.32	2.10
3	B3	3	14	1
4	B4	1.27	9	1.06
5	B5	2.4	13.8	1.10

  [a] Ductility is defined with the ratio of area under load deflection curve at ultimate load to area under load deflection curve at yield load.
  [b] K_i: initial stiffness calculated by slope of the load deflection curve before cracking.
  [c] K_u: post-cracking stiffness calculated by slope of the load deflection curve after cracking up to yielding of reinforcement.

Application of the statically based approach to the corroded rebars of the test partially prestressed concrete beams

The statically approach presented by EL-Hefnawy [4] can be used to estimate the residual minimum cross-sectional area of the corroded rebar from three random diameter measurements, and this approach can be applied to the corroded rebar of the fully prestressed beams tested and conventional concrete beam through the experimental part of the current research work. Table 6 lists the calculated probable minimum cross-sectional area of each corroded rebar of the tested conventional concrete beam and fully prestressed beam using the statically approach presented by EL-Hefnawy [4].

In attempt to verify the accuracy of EL-Hefnawy [4] statically model for estimating the minimum area of corroded rebar from measuring three random diameters along the corroded rebar length, the actual minimum bar diameters were determined for all corroded rebars of the tested beams. Hence the actual minimum cross-sectional area of corroded rebar can be computed. The actual minimum cross-sectional area of all corroded rebars of the tested beams is shown in Figs. 7 and 8.

Effect of percentage of steel reinforcement

To investigate the effect of percentage of steel reinforcement on the corroded and non-corroded conventional beams and fully bonded prestressed concrete beams, Table 7 shows the ultimate loads and the reduction percentage in load carrying capacities due to corrosion of conventional concrete beams and fully bonded prestressed concrete beams.

Corrosion-induced cracking

For the conventional concrete beam B2 the ordinary tension steel reinforcement bars was exposed to corrosion at the same time, for the same duration and under the same conditions as the remaining corroded beams. The deterioration in ordinary steel reinforcement bars as a result of the corrosion exposure leads to a reduction in cross-sectional area of the reinforcement bars. There are other associated effects caused by the buildup of corrosion products at the interface between the reinforcing bars and surrounding concrete. These corrosion products are expansive in nature and so induce radial pressures on the surrounding concrete resulting in cracking and spalling. Furthermore, the buildup of corrosion products affects the bonding between the steel reinforcing and surrounding concrete as shown in Fig. 9.

For fully bonded prestressed concrete beam B4 fully exposed to corrosion both the compression of non-prestressed steel reinforcement bars and prestressed tendon were exposed to corrosion at the same time, for the same duration and under the same conditions as the remaining corroded beams. The deterioration in bonded prestressed tendon is less likely to occur due to the complete filling of grout in the plastic duct. Conversely, the deterioration in compression of non-prestressed steel reinforced bars is more likely to corrode due to being exposed to all corrosion conditions "such as, PH level,

Table 6 The estimated minimum cross-sectional area.

Beam	Rebar no.	Rebar type							
		Non-prestressed steel rebar				Prestressed steel rebar			
		Monitored position (mm^2)			Minimum cross-sectional area (mm^2)	Monitored position (mm^2)			Minimum cross-sectional area (mm^2)
		1	2	3		1	2	3	
B2	R1	8.5	8	8.5	34.37	Not applicable			
	R2	8.0	8.6	8.3	33.32				
	R3	8.5	8.1	7.9	31.68				
	R4	8.7	8.6	8.5	49.21				
	R5	8.1	8.3	7.9	36.68				
	R6	8.4	8.6	8.7	44.92				
	R7	8.5	8.8	8.8	45.11				
B4	R1	7.5	7.5	7.6	39.90	Small effect			
	R2	7.6	7.8	7.9	36.04				
B5		Not applicable				Small effect			

chemical attack, and chloride penetration" without any protection as opposed to the protected bonded prestressed tendon. The corrosion in bonded prestressed tendons is generally due to the incomplete filling of the duct "i.e. lack grout in contact with tendon" or to penetration of chloride through defects of the sheath.

For bonded fully prestressed concrete beam B5 partially exposed to corrosion, only the prestressed tendon was exposed to corrosion at the same time, for the same duration and under the same conditions as the remaining corroded beams. The deterioration in bonded prestressed tendon is less likely to occur due to the complete filling of grout in the plastic duct. Consequently, less difference in behavior was observed in terms of ultimate capacity, crack propagation, and ductility between fully prestressed concrete beam partially exposed to corrosion B5 and fully prestressed concrete beam to non-corroded B3.

Due to the accelerated corrosion process of the beam steel reinforcement bars, horizontal cracks were observed at positions of main longitudinal steel reinforcement for conventional concrete beam B2, and in compression of longitudinal steel reinforcement for bonded fully prestressed concrete beam fully exposed to corrosion B4. The reason for this was the accumulation of corrosion products that increased the volume of reinforcement and hence developed extensive stress on the surrounding concrete. These stresses forced the concrete cover to crack. Fig. 9 shows mapping of corrosion induced cracks for specimens B2, and B4 respectively.

Modes of failure and cracking pattern

Fig. 10 shows the failure mode and cracking pattern of conventionally/fully bonded prestressed concrete beams with compressive strength 40 MPa.

Modes of failure for conventional concrete beam were more ductile than the fully prestressed concrete beams. This is attributed to the contribution of non-prestressed steel reinforcement. Failure was due to yielding of the reinforcement in tension steel bars followed by compression failure of concrete. Rupture of prestressing steel strand was observed in fully pre-

stressed concrete beams after crushing of concrete had occurred.

The cracking pattern for conventional concrete beams is distributed along the beam length and has a small crack width and high number due to the presence of non-prestressed steel, while the cracking pattern of fully prestressed concrete beams was distributed along the beam length with big crack width and few numbers due to the absence of non-prestressed steel as shown in the previous figures.
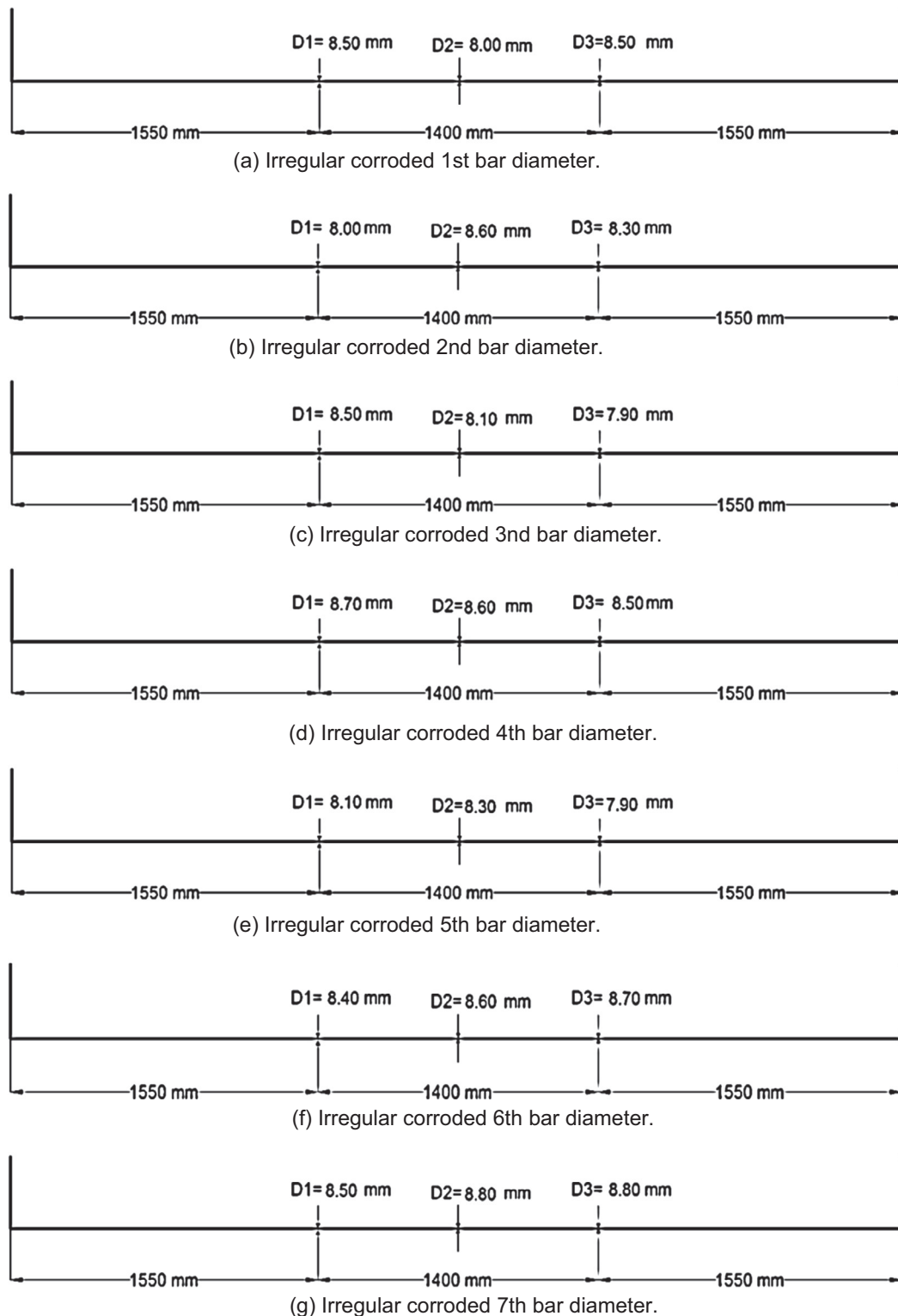
The cracking pattern for beams exposed to corrosion was similar to the control beams. In addition to the following observations, (a) the concrete color of the beams subjected to corrosion turned to brown, at the corrosion rebar zone, and (b) Irregular Cracks at concrete cover with various thicknesses have been appeared along the beam length, as shown in Fig. 11.

Discussion

In general, exposure to corrosion for all specimens at the same time duration and condition for a period of 120 days reduced the flexural capacity of the conventional concrete beams of 40 MPa compressive strength by 18.21% as shown in Fig. 12. The initial stiffness of the control beam B1 was 131.52% higher than that of beam B2. The ductility of the control beam B1 was 46.25% higher than that of beam B2 as shown in Fig. 13. These differences in the stiffness and ductility are attributed to the corrosion of steel.

Exposure to corrosion reduced the flexural capacity of the fully prestressed concrete beams B4 (fully exposed to corrosion) and B5 (partially exposed to corrosion) of 40 MPa compressive strength by 10% and 5%, respectively, as shown in Fig. 14. The initial stiffness of the control beam B3 was 55.55% and 1.5% higher than those of beams B4, and B5, respectively. The ductility of the control beam B3 was 136% and 15.4% higher than those of beams B4, and B5, respectively as shown in Fig. 15. These differences in the stiffness and ductility are attributed to the steel corrosion.

The abilities of fully bonded prestressed concrete beams to resist the corrosion are higher than those of the conventional

D1= 8.50 mm   D2= 8.00 mm   D3=8.50 mm

1550 mm   1400 mm   1550 mm

(a) Irregular corroded 1st bar diameter.

D1= 8.00 mm   D2=8.60 mm   D3= 8.30 mm

1550 mm   1400 mm   1550 mm

(b) Irregular corroded 2nd bar diameter.

D1= 8.50 mm   D2=8.10 mm   D3=7.90 mm

1550 mm   1400 mm   1550 mm

(c) Irregular corroded 3nd bar diameter.

D1= 8.70 mm   D2=8.60 mm   D3= 8.50mm

1550 mm   1400 mm   1550 mm

(d) Irregular corroded 4th bar diameter.

D1= 8.10 mm   D2=8.30 mm   D3=7.90 mm

1550 mm   1400 mm   1550 mm

(e) Irregular corroded 5th bar diameter.

D1= 8.40 mm   D2=8.60 mm   D3= 8.70 mm

1550 mm   1400 mm   1550 mm

(f) Irregular corroded 6th bar diameter.

D1=8.50 mm   D2=8.80 mm   D3= 8.80 mm

1550 mm   1400 mm   1550 mm

(g) Irregular corroded 7th bar diameter.

Fig. 7   Irregular corroded bars diameter for specimen B2.

concrete beams in terms of flexural capacity and initial stiffness. This is attributed to using bonded prestressed tendon in fully prestressed concrete beams, where the deterioration in bonded prestressed tendon is less likely to occur due to complete filling of grout in the plastic duct. Conversely, the deterioration in non-prestressed steel reinforcement bars in conventional concrete beams, is more likely to corrode due to being exposed to all corrosion conditions. The increase in
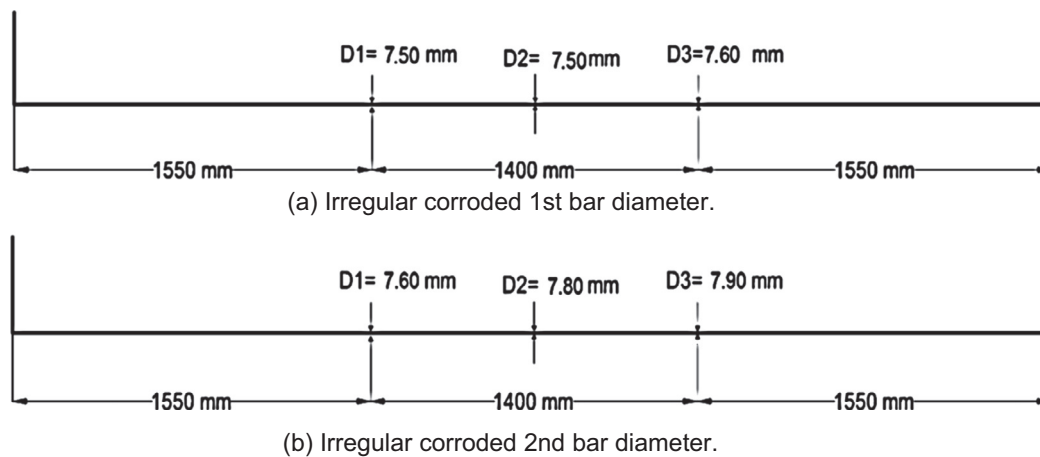
(a) Irregular corroded 1st bar diameter.

(b) Irregular corroded 2nd bar diameter.

Fig. 8   Irregular corroded bars diameter for specimen B4.

Table 7   Effect of percentage of steel reinforcement on conventional and fully bonded prestressed beam capacities.

Type of beams	Beam	Ultimate load	The percentage of steel reinforcement[a] (%)	Reduction percentage	Time of corrosion process
Conventional concrete beams	B1	130.00	0.916	–	120 days duration
	B2	106.32	0.459	18.21	along beam length
Fully prestressed concrete beams	B3	123.80	0.261	–	
	B4	111.36	0.126	10.00	
	B5	117.27	0.261	5.00	

[a] Based on EL-Hefnawy [4] statically approach.
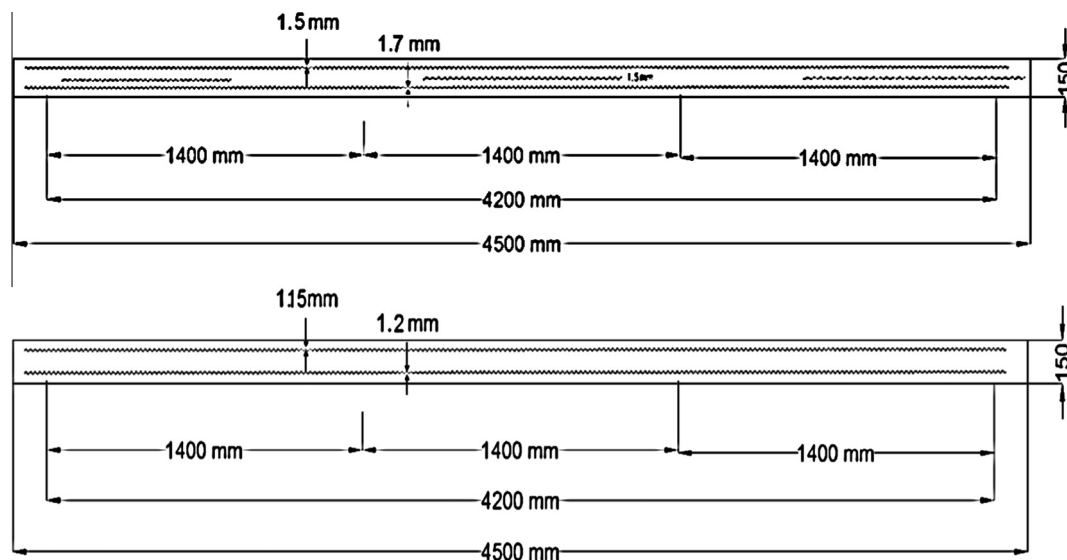
Fig. 9   Mapping of stress crack corrosion for specimens B2, and B4.

the ductility for conventional corroded beam is attributed to the presence of non-prestressed reinforcement steel bars which controlled the crack formation and reduced the crack width.

The difference in flexural capacity between the fully and partially corrosion exposed for prestressed concrete beams of 40 MPa compressive strength was 5%. This slight difference can be attributed to the damage of the bonded prestressed strand against the corrosion not being observed. This is due to the use of grout to completely fill the gaps around the prestressed strands inside plastic duct preventing corrosion as a result of the chemical attack and chloride penetration.

Fig. 10   Crack pattern and failure for specimens.

Fig. 11   The deterioration of the concrete against corroded rebar for samples.

The anchorages and end stubs of strands should be carefully protected. Although anchorage corrosion can lead to failure of the anchorage, the bond between the tendon and concrete will prevent a complete loss of prestress force. Corrosion of the anchorage hardware can lead to cracking and spilling of the concrete near the anchorage, and also allows moisture to enter the duct causing subsequent tendon corrosion.
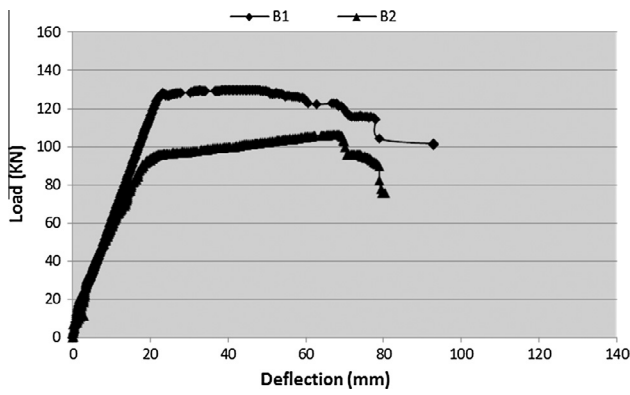
Fig. 12   Load-mid span deflection relationship for B1 and B2.
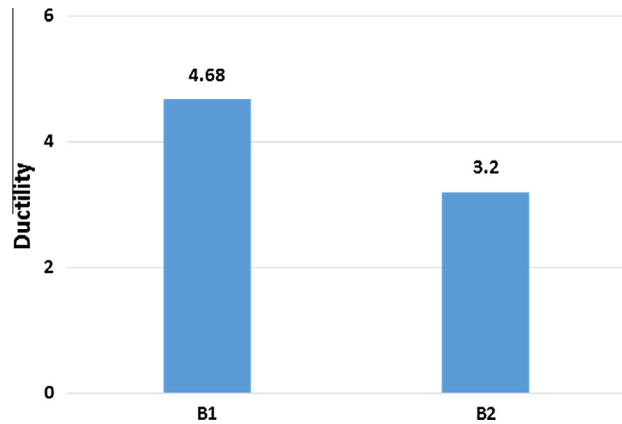
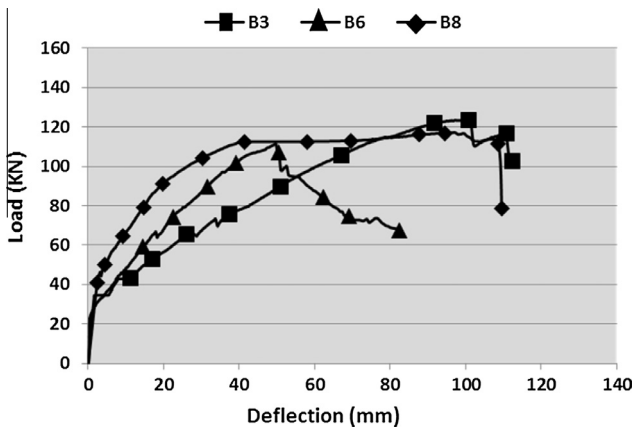Fig. 13   Ductility for B1 and B2.

Fig. 14   Load-mid span deflection relationship for B3, B4 and B6.

Analytical study

Analysis of the tested specimens was carried out to predict the deformational behavior of fully bonded prestressed concrete beams. Deflection and curvatures at the mid-span sections were calculated. Concrete was modeled using a parabolic
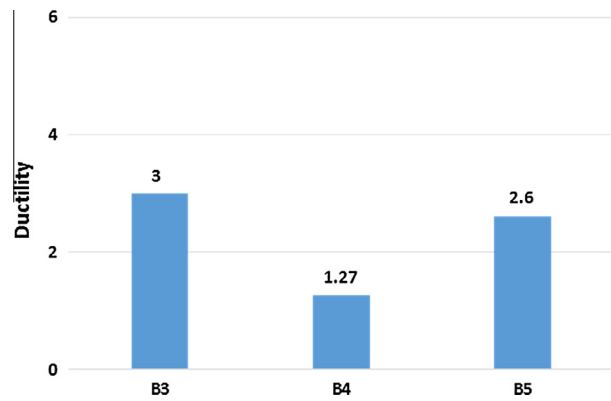

Fig. 15   Ductility for B3, B4, and B5.

stress–strain curve, while steel was modeled using a bilinear stress–strain relationship. Strain compatibility and force equilibrium were carried out using an iterative process to establish the moment–curvature relationship at each section. For each load increment, the curvature at different sections along the length of the beam was determined. Maximum deflection of the beam was calculated by integration of the curvature from the support section to the mid-span section under the specified incremental load. The stress–strain relationship for the strands is taken into account according to the formula presented by Tadros and Devalapura [11].

$$f_{ps} = \varepsilon_{ps} \left[A + \frac{B}{\left\{ 1 + (C\varepsilon_{ps})^D \right\}^{\frac{1}{D}}} \right] \leqslant f_{pu} \qquad (1)$$

where

f_p = stress in the steel strand;
ε_{ps} = strain the steel strand;
f_{pu} = ultimate stress in the steel strand and
$A = 384$, $B = 27{,}616$, $C = 119.7$, and $D = 6.43$ (formula constants)

According to EL-Hefnawy approach to use the proposed computer program, some site measurements must be first determined, select three different positions along the rebar length and measure the diameter at each of these positions as shown previously in Figs. 7–10, and used to estimate the probable minimum area of the corroded rebar (AF) as shown the following formula and used as input data on analytical program [4]:

a. Compute the mean and the standard deviation for the three areas for which the diameters were measured (R (x)).

$$\text{Mean area} = AR = \frac{1}{4} * \sum_{x=1}^{4} R(x) \qquad (2)$$

b. Compute the derived mean and the derived standard deviation.

The derived mean = $U = AR$.

$$\text{Standard deviation} = SD = \sqrt{\frac{1}{3} * \sum_{x=1}^{4} (AR - R(x))^2} \qquad (3)$$

The derived standard deviation $= SM = 1.48 * SD$ (4)

c. Compute the coefficient of variation.

Coefficient of variation $= CV = \dfrac{SM}{U}$ (5)
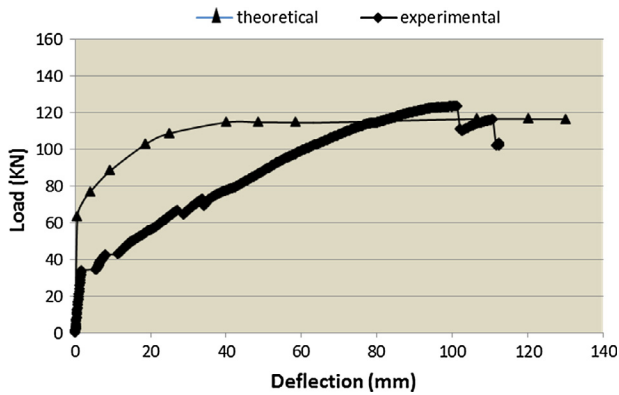
d. Calculate the partial safety factor.

Partial safety factor $= SF = (4.5 * CV) + 1$ (6)
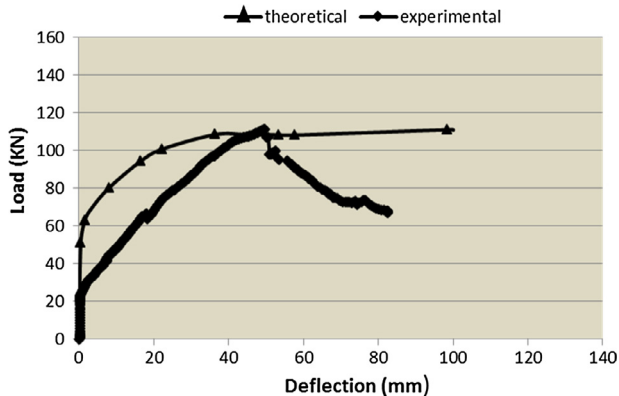
e. Calculate the characteristic area.

Characteristic area $= AK = U - 1.64\ SM$ (7)

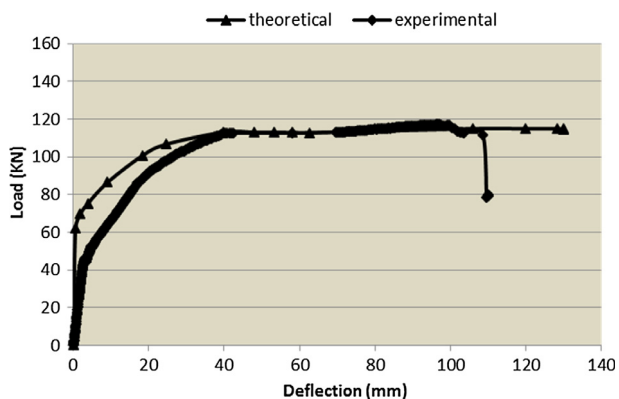f. Finally, calculate the probable minimum area of the corroded rebar.

Probable minimum area $= AF = \dfrac{AK}{SF}$ (8)

A very good correlation between the predicted and measured behavior was observed and is presented in Fig. 16.

Conclusion

From the analysis and discussion of the test results obtained from this research, the following conclusions can be drawn:

1. The presence of prestressed force in fully bonded prestressed concrete beam led to a slight decrease in ultimate flexural capacity due to corrosion up to 10%, while 18.21% decrease in ultimate flexural capacity due to corrosion of conventional concrete beam.
2. The presence of prestressed force in fully bonded prestressed concrete beam delays the concrete cracking and increases the initial stiffness up to 40% compared with that of conventional concrete beam.
3. The presence of non-prestressed reinforcement in conventional concrete beam enhanced the ductility up to 56% compared with that of fully bonded prestressed concrete beams, and improved the serviceability of the beams by controlling the crack formation and decreasing the crack width and distributing it along beam length.
4. Most of deterioration due to corrosion incident in conventional concrete beam and fully bonded prestressed beam act on non-prestressed reinforcement. Because the bonded tendons are less likely to corrode. Occurrence of corrosion for bonded prestressed steel strand is so complex and is influenced by many factors. This is often referred to providing multilevel protection for prestressed strand; cement grout acts as a barrier to both moisture and chloride penetration and produces an alkaline as well. Same goes for duct which plays the same role of cement grout, especially plastic duct without splice and connections.
5. The theoretical analysis based on strain compatibility and force equilibrium gave a good prediction of the deformational behavior for fully bonded prestressed concrete beams.

(a) Theoretical and Experimental result Load-Deflection Curve for sample B3.

(b) Theoretical and Experimental result Load-Deflection Curve for sample B4.

(c) Theoretical and Experimental result Load-Deflection Curve for sample B5.

Fig. 16   Theoretical and experimental curves of fully bonded prestressed concrete beam.

Conflict of interest

The authors declared that there is no conflict of interest.

References

[1] F.H. Omnia, Behavior of Fully and Partially Prestressed Concrete Beams with Different Compressive Concrete Strength, PhD Thesis, Ain Shams University, 2012.
[2] A.M. Ismail, Behavior of Statically Determinate Prestressed Concrete Beams Subjected to Fire, PhD Thesis, University of Ain Shams, 2011.

[3] A.A. EL-Hefnawy, Some Durability Aspects of Concrete in Absence of Silica Fume, MSc Thesis, Cairo University, 1995.

[4] A. El-Hefnawy, A New Statistical Approach for Predicting the Residual Capacity of Reinforced Concrete Beams Having Corroded Main Steel, PhD Thesis, Cairo University, 2000.

[5] International Standard, Statistical Methods for Quality Control of Building Materials and Components, ISO 12491:1997 (E), first ed., Switzerland, May 1997.

[6] E. Gestsdottir, T. Gudmundsson, Bond Behavior of Naturally Corroded Reinforcement in Concrete Structures, Master of Science Thesis in the Master's Program Structural Engineering and Building Performance Design, CHALMERS University of Technology, Göteborg, Sweden, 2012.

[7] T.S. AL-Attar, M.S. Abdul-kareem, Effect of chloride ions source on corrosion of reinforced normal and high performance concrete, Bull. AGIR 02 (2011) 107–112 (April–June).

[8] M. Khafaga, T. Bahaa, Structural behavior of reinforced concrete beams deteriorated due to corrosion of web reinforcement, in: International Conference: Future Vision and Challenges for Urban Development Cairo, Egypt, 20–22 December 2004.

[9] A. Elgabry, M. Hilal, H. Bahnasawy, M. El-Attar, Rehabilitation of Corroded Reinforced Concrete Frames Using CFRP Sheets, Structural Composites for Infrastructure Applications, Alexandria, Egypt, May 2005.

[10] E.C.P. Egyptian Code of Practice for Reinforced Concrete Construction, Ministry of Development, New Communities, Housing and Utilities, Housing and Building National Research Center, 2007.

[11] M.K. Tadros, R.K. Devalapura, Stress–strain modeling of 270 ksi low-relaxation prestressing strands, PCI J. 37 (1992) 100–106 (March–April).